Time-Delay Measurements from Antarctic Neutron Monitor Stations Indicate Weak Spectral Changes during 27-day Variations

Pradiphat Muangha,[a,*] **David Ruffolo,**[a] **Alejandro Sáiz,**[a] **Chanoknan Banglieng,**[a,b] **Paul Evenson,**[c] **Surujhdeo Seunarine,**[d] **Suyeon Oh,**[e] **Jongil Jung,**[f] **Marc Duldig**[g] **and John Humble**[g]

[a]*Mahidol University, Department of Physics, Bangkok 10400, Thailand*

[b]*Rajamangala University of Technology Thanyaburi, Division of Physics, Faculty of Science and Technology, Pathum Thani 12110, Thailand*

[c]*University of Delaware, Department of Physics and Astronomy, Newark, DE 19716, USA*

[d]*University of Wisconsin, River Falls, WI 54022, USA*

[e]*Chungnam National University, Department of Astronomy, Space Science and Geology, Daejeon 34134, Korea*

[f]*Chonnam National University, Department of Earth Science Education, Gwangju 61186, Korea*

[g]*University of Tasmania, School of Natural Sciences, Hobart, Tasmania 7001, Australia*
E-mail: fhoone@hotmail.com, david.ruf@mahidol.ac.th, alejandro.sai@mahidol.ac.th, evenson@udel.edu, surujhdeo.seunarine@uwrf.edu

Using neutron time-delay data from neutron monitors (NMs), we can extract the leader fraction, L, of neutron counts that do not follow a previous neutron count in the same counter tube due to the cosmic ray shower. L is the inverse of the neutron multiplicity and serves as a proxy of the cosmic ray spectral index over the rigidity range of the NM response function. We have outfitted several Antarctic NMs with special electronics to collect neutron time delay distributions. We present a comparative analysis of L during two time periods: 1) during December 2015 to January 2017, for NMs at South Pole (SP), McMurdo (MC), and Jang Bogo (JB), and 2) during February 2020 to February 2021, for NMs at SP, JB, and Mawson (MA). To first order L varies in concert with the count rate C, reflecting unrolling of the Galactic cosmic ray (GCR) spectrum as part of solar modulation during the declining phase of solar cycle 24 and during solar minimum. However, during 27-day variations in C due to high-speed solar wind streams (HSSs) and corotating interaction regions (CIRs), L usually had a very weak variation. Our results indicate weak GeV-range GCR spectral variation due to HSSs and CIRs, relative to the flux variation, in contrast with the strong observed spectral variation due to solar modulation.

*37*th *International Cosmic Ray Conference (ICRC 2021)*
July 12th – 23rd, 2021
Online – Berlin, Germany

---

*Presenter

1. Introduction

Neutron monitors (NMs) are ground-based detectors of secondary particles produced in atmospheric cascades from primary cosmic ray ions. NMs consist of several proportional counters (mainly filled with BF3 or 3He gas), which are sensitive to the neutrons produced by the interaction of the secondary particles with a dense lead producer. Monitoring the count rate C provides information about variations of the cosmic ray flux entering at the top of the atmosphere due to the solar modulation, in particular the long term modulation (with the 11 year sunspot cycle and the 22 year solar magnetic cycle) as well as the short term variations (the Forbush decreases from solar activity and the rotation period of the ~27-day and daily variation related to the solar rotation and the Earth's rotation, respectively).

By using the specialized electronics were designed to record neutron time-delay histograms. The techniques to remove the effect of chance coincidences and extract the "leader fraction" L of neutron monitor count that did not follow other counts in the same counter tube from the same cosmic ray shower were also developed in the previous work as shown in [1]. This work mainly focus on a comparative analysis of L during two time periods: 1) during December 2015 to January 2017, for NMs at South Pole (SP), McMurdo (MC), and Jang Bogo (JB), and 2) during February 2020 to February 2021, for NMs at SP, JB, and Mawson (MA). we present observations of the 27-day variations in C much stronger than L examine the relationship between the 27-day GCR variations and heliospheric parameters.

2. Neutron monitor time-delay histograms

Using neutron time-delay data from a single station with specialized electronics, we can indicate variations in the cosmic-ray spectral index [1]. The South Pole NM (SP), at an altitude of 2828 meter, has three 1NM64 detectors. The SP NM started using these electronics on NM tubes to recorded the time-delay histograms in 2013 December and the complete set of 3 counter tubes in 2015 March. For each of the three tubes, the electronics provided hourly time delay histograms with different time scales. For more details about the experimental determination of the time-delay histograms, we refer to [1]. The long time histogram presents an exponential tail represent the coincidence time delay distribution between two uncorrelated incoming secondary particles (mostly neutrons) while The short time-delay histogram shows the nonexponential that can be attributed to the time delays between neutron counts that originated from the same lead nucleus in the same secondary particle.

Jang Bogo (JB) station at latitude -74.6°N, longitude 164.2°E, and altitude 48 m, which located close to McMurdo (MC) station at latitude -77.9N, longitude 166.6E, and altitude 30 m, was installed neutron monitor on 5 NMs in December 2015 [4]. The MC station was close in January 2017. Around January 2019, 12 NM tubes from MC station moved to JB station, which use these electronics on 6 tubes. Then JB have 11 NM tubes that can collect time delay histogram. During December 2015 to January 2017, MC station used these electronics on 6 NM tubes.

Neutron monitors at Mawson (MW) station, where located at sea level, at latitude -67.6°N, longitude 62.8°E, was installed the data acquisition system included both updated electronic firmware to be able to measure time-delay histograms in early February 2020 for 18 NM tubes.

2.1 Extraction of the leader fraction

The leader fraction L, defined as the fraction of neutron counts that did not follow a previous neutron count in the same tube from the same atmospheric secondary, which is inversely related to the multiplicity as a proxy of a GCR spectral index above the cutoff. We refer to [1] that it is possible to extract the leader fraction L from each time delay histograms i.e., for each counter tube and each time interval. They also developed methods to statistically remove the effect of chance coincidences to extract the leader fraction.

When the secondary particles interact in the NM producer (mostly in the lead), a harder spectrum should lead to produceing more neutrons with a greater multiplicity and a lower leader fraction. Therefore, a lower leader fraction is associated with a harder cosmic-ray spectrum with a lower spectral index. [1] showed that the leader fraction at Doi Inthanon can indicate short-term spectral variations. Note that NM count rates are always corrected for pressure variation, and the leader fraction L has been found to vary with P as well. The pressure corrected L for each counter tube is different, mainly due to its position and electronic dead time.

3. Observations

3.1 Comparative analysis of leader fraction

Here we present the variation of the GCRs count rate and L. Because atmospheric secondary particles are rapidly absorbed in the atmosphere, NM count rate is generally corrected for barometric pressure, which provides a measure of the air mass above the detector. The leader fraction L is quite sensitive to the energy of secondary nucleons (see Figure 10 of [3]) With high pressure, more energetic secondary particles are less likely to survive and increase L value (higher multiplicity). Because of that the pressure has a positive correlation with L, in contrast with the negative correlation with C [2].

South Pole NM record particularly highest count rates, about 300 counts/sec, correlated with lowest L, about 0.75, (Figure 1) because SP at high altitude and other station at sea level. Figure 1(a) presented period in December 2015 to January 2017, where SP, JB, and MC data collected at the same period. JB and MC NM are well correlated and have similar values of C and L (about 270 counts/sec and o.83 for C and L repectively) because these two stations are close to each other. Figure 1(b) show count rate and L during February 2020 to February 2021, where SP, JB, and MA data ware present at the same period. MA station is higher L (about 0.84) corresponding lower NM count rate (about 260 counts/sec). NM count rates were clearly see 27-day modulation while L were small variation (figure 1(a)). i.e. Around late 2015, both SP count rate and L were strongly 27-day variation. Around June 2016, SP, JB, and MC count rates ware clearly see 27-day variation but L ware not. The jump in JB leader fraction due to changing software version (Landmonitor version) on April 29, 2020.

3.2 Periodic of the variation of GCR, leader fraction, and heliospheric parameters

We used data of the neutron monitors located at South Pole, Jang Bogo, McMurdo, and Mawson, which have geomagnetic cutoff rigidities of $R_c < 1$ GV, so the detector response is determined by an atmospheric cutoff at ~1 GV. The pressure-corrected data of the GCR count rate
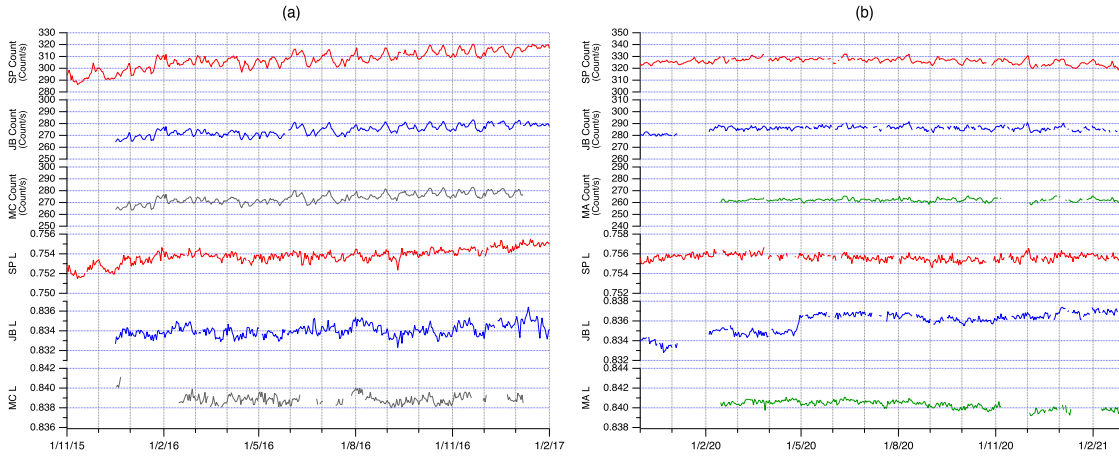
Figure 1: (a) Comparison of daily averaged count rates from 2015 December to 2017 February from the South Pole, Jang Bogo, and McMurdo NMs. Each NM count rate has the same trend. Variations in the leader fraction *L* generally indicate changes in the cosmic-ray spectrum. **(b)** Comparison of daily averaged count rates from 2020 February to 2021 February from the South Pole, Jang Bogo, and Mawson NMs.

C and *L* were detrended as $\delta\mathrm{I}[\%] = 100 \times (x_i - \bar{x})/\bar{x}$ to remove the longer-term variations in solar modulation, where *x* is daily average NM data, *C* or *L* and $\bar{x}$ the 27-h moving-average. Relative detrended count rate and *L*, daily average, are present for GCR count rate *C* and spectral change *L* in Figure 2 with detrend solar parameters, solar wind velocity and HMF magnitude, respectively including the *Br* component of HMF. These solar parameters were obtain from OMNI2 data: (https://spdf.gsfc.nasa.gov/pub/data/omni/).

Figure 2 illustrates the 27-day variations present in neutron monitor rates and leader fraction *L* during the March 2015 to February 2017 (left) and July 2018 to June 2020 (right), compared with detrended solar wind speed and magnetit field magnitude over 27-day. These "detrended" data show an intensity fluctuation of about zero. Count rate *C* peaks occur mostly near the same time in all the cosmic ray rates, corresponding with minima in the solar wind speed, which occur at magnetic sector crossings in the slow speed wind. There are strong two peaks in the solar wind (SW) speed during late of 2016 figure 2 (middle) corresponding with two peaks in *C* but not clear variation in *L* (mostly one peak with weak variation). Time lines of the 27-day variations in *L* is mostly similar in shape to *C* but weak observed. In figure 2 (right), both *C* and *L* were weaker 27-day variation than figure 2 (left) correlated to weaker variation in solar wind speed, and the heliospheric magnetic field (HMF).

To study the temporal changes of the periodicity variation that connected with the Sun's rotation, we analyze the relationship of quasi-periodic variations of *C*, *L*, and heliospheric parameters using the wavelet analysis. In Figures 3 we present results of wavelet analysis: South Pole count rate *C* [%], South Pole leader fraction *L*[%], HMF magnitude (B) [%], and Br component of HMF [nT], respectively. The count rate *C* are mostly see two significance signals with periodicities of ~27 days and ~13 days that are mostly similar to the solar wind velocity. *L* seem to be correlated with *C* in ~ 27-day periodicity but weak in the periodicity of 2nd harmonic (~ 13 days). For example, during late 2016, SW data show a strong half period of solar rotation. It mean two part of the solar
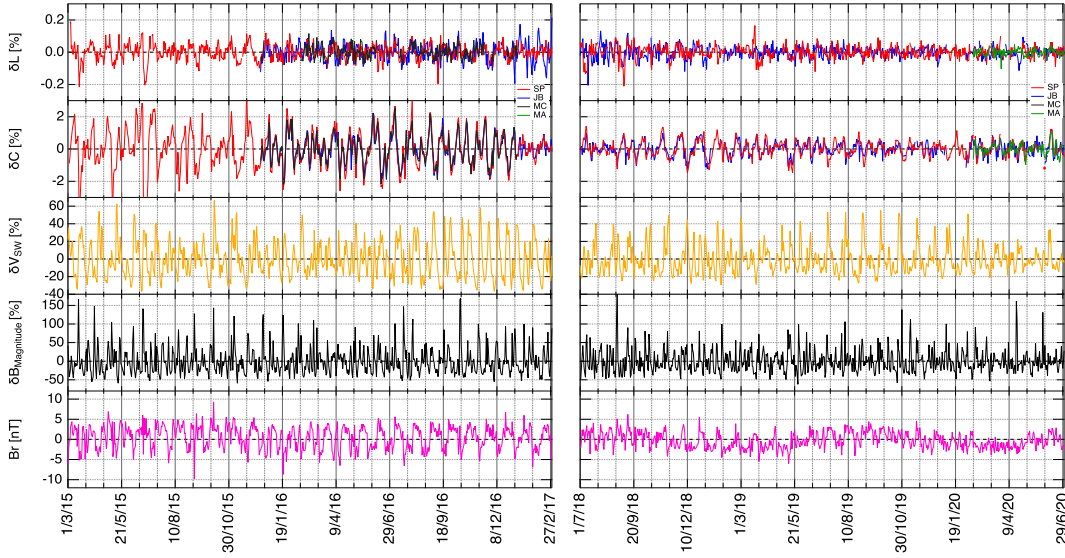
Figure 2: Daily NM count rate *C*, *L*, solar wind velocity, HMF magnitude normalized and detrended over 27-days smoothing, and the daily *Br* component of HMF for March 2015 to February 2017 (left) and July 2018 to June 2020 (right).

surface leading strong solar wind but one of them affects the spectrum. The other one apparently does not because L has one period instead of two. The B_r component of HMF exhibited strong variation with a 27-day period and clearly exhibited the ~13-day period. So, the spectral variation show only 27-day period but not a harmonic.

3.3 Characteristic features of 27-day variations in GCR and *L*

As we considered the relationship between the 27-day variation in GCR count rates and *L* with solar wind and plasma parameters. The comparative detrended of daily average deviation from the 27-day averages for each station of neutron monitor data (*C* and *L*) with the detrended solar wind speed and magnetic field strength. Results show *C* and *L* are significant correlated with the solar wind speed than magnetic field magnetic field magnitude, Figure 4 as a sample of SP station. The significant correlation define as the linear fit coefficient of the detrended of *C* and *L* versus the detrended of SW and B magnitude greater than two-sigma of the slope. The coefficients for each station follow: C_{SP} vs SW_s is $-1.43E-02 \pm 9.17E-04$, C_{SP} vs B_{mag} is $-5.74E-04 \pm 4.23E-04$, L_{SP} vs SW_s is $-4.38E-04 \pm 5.06E-05$, L_{SP} vs B_{mag} is $-2.92E-05 \pm 2.27E-05$, C_{JB} vs SW_s is $-9.99E-03 \pm 8.07E-04$, C_{JB} vs B_{mag} is $-3.15E-04 \pm 3.64E-04$, L_{JB} vs SW_s is $-2.29E-04 \pm 7.05E-05$, L_{JB} vs B_{mag} is $-1.60E-05 \pm 3.05E-05$, C_{MC} vs SW_s is $-2.13E-02 \pm 1.89E-03$, C_{MC} vs B_{mag} is $-7.06E-05 \pm 1.02E-03$, L_{MC} vs SW_s is $-4.68E-04 \pm 1.13E04$, L_{MC} vs B_{mag} is $3.12E-06 \pm 5.97E-05$, C_{MA} vs SW_s is $-5.43E-03 \pm 1.29E-03$, C_{MA} vs B_{mag} is $8.55E-04 \pm 5.39E-04$, L_{MA} vs SW_s is $-2.58E-04 \pm 0.80E-04$, L_{MA} vs B_{mag} is $1.74E-05 \pm 3.38E-05$. These correlation coefficients imply that the time behavior in the period of 27-day variation in GCR count rate and L are mainly effect by solar wind speed. Moreover, there is less correlation between deviations from the averages of magnetic field magnitude. Note that we
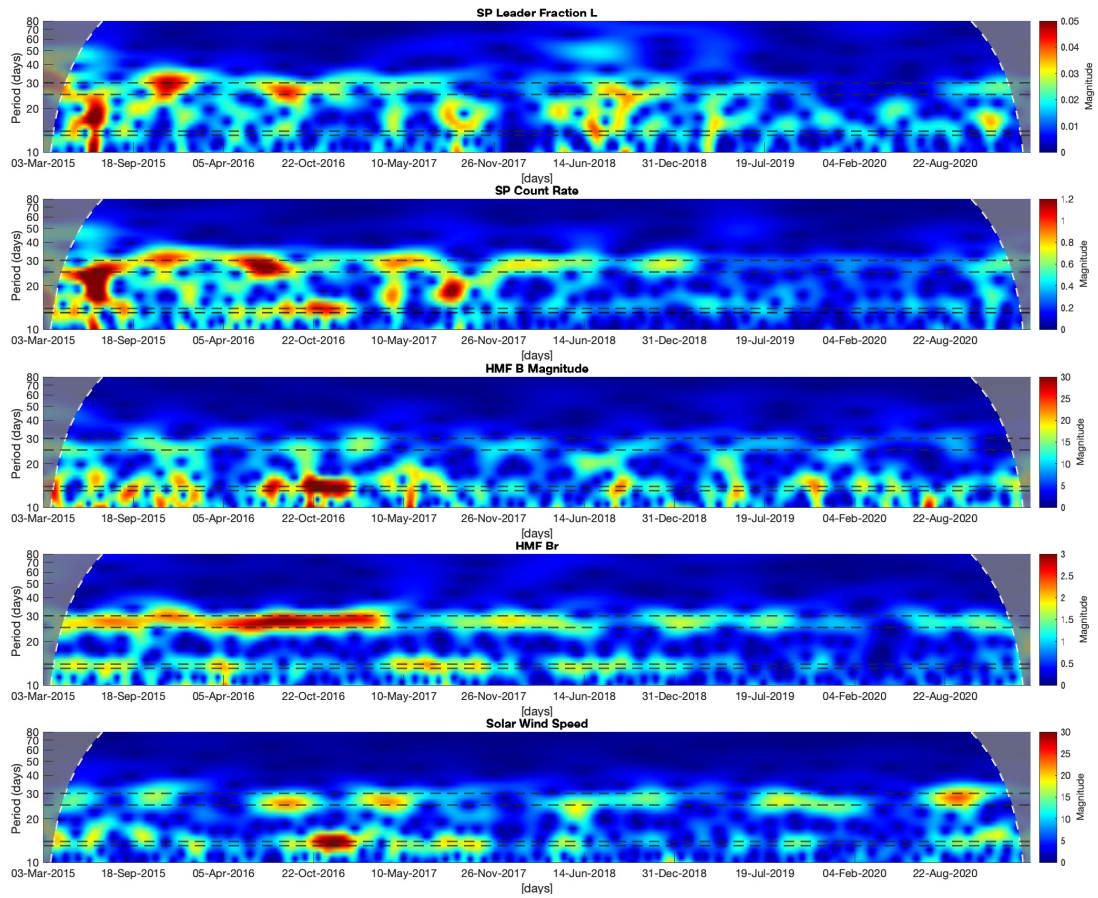
Figure 3: Wavelet analysis of daily SP *C*, *L*, the magnetic field magnitude of HMF, the *Br* component of HMF, and solar wind speed for March 2015 to February 2021. White dashed line corresponds to the 95% confidence level. Horizontal black dashed lines for each panel corresponds to the period of 30-day, 25-day, 14-day, and 13-day, respectively.

use data from December 2015 - February 2021 for SP and JB, December 2015 - January 2017 for MC, and February 2020 - February 2021 for MW.

As a case study we consider the 27-day variation of the GCR intensity, solar wind velocity and the magnetic field during January 2016 – January 2017 corresponding to the Bartels'rotations (BR) 2489-2502(Fig. 2 (a)) and February 2020 – February 2021 BR 2545-2558 (Fig. 2 (b)) We consider as an example average data of these 13 BR. Figure 5 present the characteristic features of the 27-day variations in terms of *C* and *L* with solar wind speed and magnetic field magnitude averaged, which superimposed by means of 13 BR, temporal changes of the daily average data relative to variation average value for 27-day running average. The double peaks in SW are not seen in GCR intensity and *L* as the same percentage. The decrease in the solar wind speed clearly correlate with the enhancement in *C* and *L*. The changing in *C* was ∼ 20 times higher than *L*.

We consider the correlation between *C* and *L* variation in each Bartel's rotation (BR). The daily average *L* versus daily average *C* of BR 2496 show as sample in figure 6 with linear fit for SP, JB, and MC stations. By apply these slope of each BR, results show in Figure 7. The slope present the correlation between *L* and *C*. The high slope correspond large change in *L* and *C* in

6
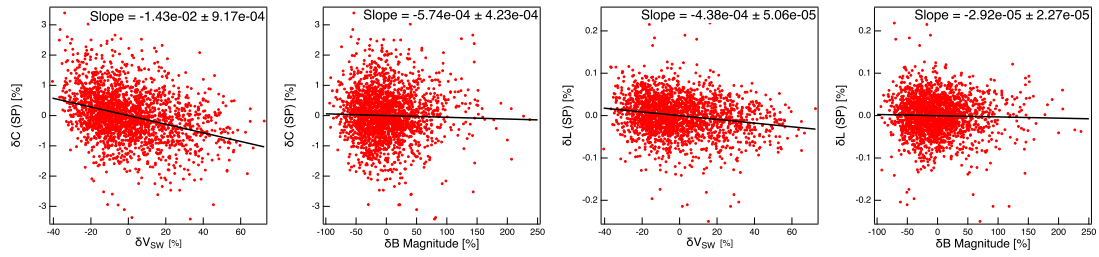
Figure 4: Percent differences between the daily-averaged values and the 27-day running averages of the South Pole neutron monitor rate versus the analogous percent differences in the solar wind speed and in the magnetic field magnitude during the period March 2015 - February 2021
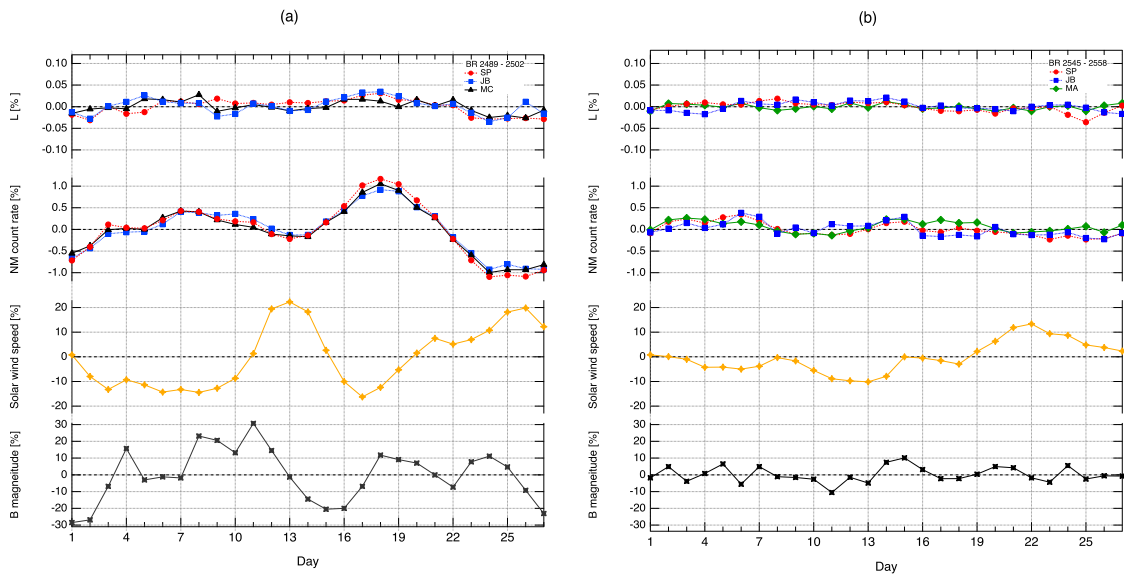

Figure 5: (a) Temporal changes of the daily solar wind velocity at the Earth orbit (points) superimposed by means of 14 BR (2489 to 2502). **(b)** The same as **(a)** but 14 BR (2545 to 2558)

27-day with the clearly peak of solar wind speed. That mean spectral changing corresponding with count rate. In contrast, lower slope indicate variation in GCR count rate but not change spectrum. In addition, the small variation in GCR count rate show low statistics in slope during 2020. Four NM stations mostly have the same trend of the modulation of GCR count rate and spectrum.

4. Acknowledgments
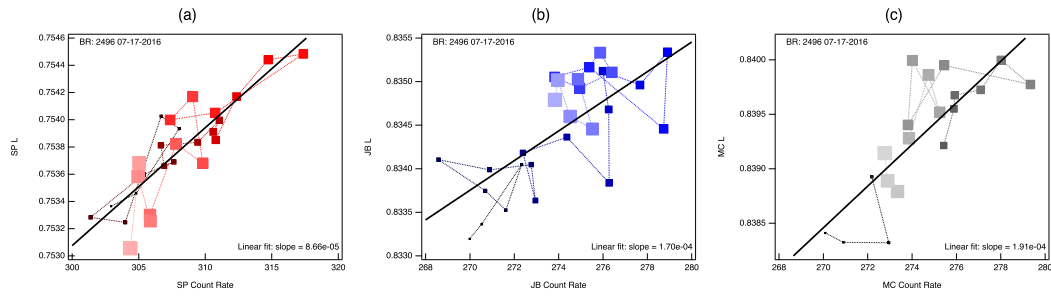
Figure 6: Daily average in leader fraction versus count rate (in count/sec) at South Pole **(a)**, Jang Bogo **(b)**, and McMurdo **(c)** during Bartel's rotation 2496.
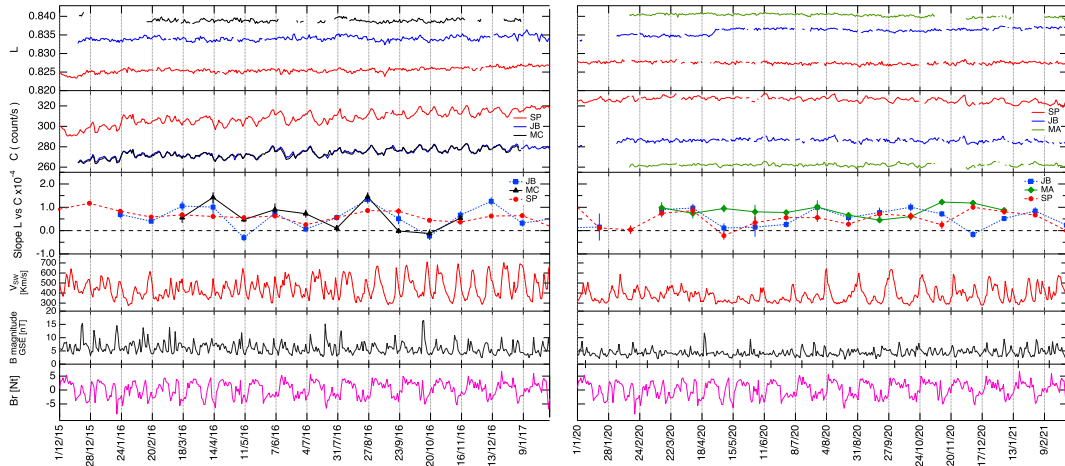
Figure 7: 27-day averaged in leader fraction *L*, NM count rate *C*, linear slope of *L* versus *C* for each BR, solar wind speed, magnetic field magnitude, and the *Br* component magnetic field. Note that SP *L* was offset y-scale by multiply 1.09 to shift SP *L* to close with other NM station data.

References

[1] D. Ruffolo et al., *Monitoring Short-term Cosmic-ray Spectral Variation Using Neutron Monitor Time-delay Measurements*, *Astrophys. J.*, 817, 38, 2016.

[2] C. Banglieng et al., *Tracking Cosmic-Ray Spectral Variation during 2007–2018 Using Neutron Monitor Time-delay Measurements*, *Astrophys. J.*, 890, 21, 2020.

[3] P.-S. Mangeard et al., *Dependence of the neutron monitor count rate and time delay distribution on the rigidity spectrum of primary cosmic rays*, *J. Geophys. Res. Space Physics*, 121, 11620, 2016a.

[4] J Jung et al., *Installation of Neutron Monitor at the Jang Bogo Station in Antarctica*, *J. Astron. Space Sci.*, 33(4), 345-348, (2016)a.